

ACCOUNT

NOVA
Publishers

VIEW CART

[Home](#) [Books](#) [Series](#) [Journals](#) [Reference](#) [eBooks](#) [Information](#) [Sales](#) [Imprints](#) [for Authors](#)
[Top](#) » [Catalog](#) » [Books](#) » [Chemistry including Chemical Engineering](#) »

[My Account](#) | [Cart Contents](#) | [Checkout](#)

Quick Find

Use keywords to find the product you are looking for.
Advanced Search

What's New? 

Advances in Materials Science
Research. Volume 9
\$95.00

Shopping Cart 

0 items

Information

[Shipping & Returns](#)
[Privacy Notice](#)
[Conditions of Use](#)
[Contact Us](#)

Bestsellers

01. Inorganic Biochemistry: Research Progress
02. Electroanalytical Chemistry Research Developments
03. New Trends and Potentialities of ToF-SIMS in Surface Studies
04. Nitrogen Fixation Research Progress
05. Clinical Chemistry Research
06. Biochemistry and Chemistry: Research and Development
07. Biodiesel: Blends, Properties and Applications
08. Chemical Engineering Research Trends
09. Green Composites: Properties, Design and Life Cycle Assessment
10. Living and Controlled Polymerization: Synthesis, Characterization and Properties of the Respective Polymers and Copolymers.

Notifications 

Notify me of updates to **Wavelets: Classification, Theory and Applications**

Tell A Friend

Tell someone you know about this product.

Wavelets: Classification, Theory and Applications

Retail Price: ~~\$165.00~~

10% Online Discount
You Pay: \$148.50

Editors: Manel del Valle (Universitat Autònoma de Barcelona, Bellaterra, Spain), Roberto Muñoz Guerrero and Juan Manuel Gutierrez Salgado (CINVESTAV, Mexico City, Mexico)

Book Description:

This book presents an integrated view of the current use of wavelets in science and engineering. This tool has been used substantially in many different application fields, especially for identification or classification purposes. Various authors from around the world have collaborated in this edited collection. The book opens with an introduction of the involved theoretical concepts, starting with the applications related to image processing. Applications in the fields of biology, food, agriculture and environment are included, as well as the medical and chemical uses of wavelets. (Imprint: Nova)

Table of Contents:

Preface

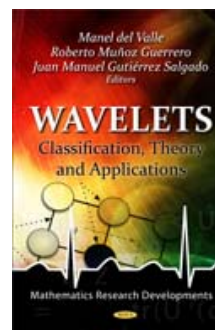
Chapter 1. Applications of Wavelet Transform;pp. 1-32
(Vipula Singh, Electronic and Communications Dept. Bangalore, India)

Chapter 2. Processing Applications of Quaternion Atomic Function Wavelets Using the Phase Concept;pp. 33-42
(E. Ulises Moya-Sánchez and Eduardo Bayro-Corrochano, Dept. of Electrical Engineering and Computer Science, Campus Guadalajara, Mexico)

Chapter 3. The Multiresolution Wavelet-Based Transformation of 3D Object Surface Meshes;pp. 43-65
(Agnieszka Szczesna, Silesian University of Technology, Institute of Informatics,Poland)

Chapter 4. Autocorrelation Removal for Spatial Statistical Modelling and its Application to Biogeographical Data;pp. 67-96
(Gudrun Carl and Ingolf Kühn,Hemholtz Centre for Environmental Research, Dept. of Community Ecology,Germany)

Chapter 5. Wavelets and Clustering: Methods to Assess Synchronization;pp. 97-124
(Irene L. Hudson, Marie R. Keatley and In Kang,University of



Click to enlarge

Special Focus Titles

01. Pedagogy of Power, Oppression and Empowerment: A Chinese Cultural Articulation
02. Opportunity, Strategy & Entrepreneurship: A Meta-Theory Vol. 2. The Sources of Opportunity, Resources, Skills, Competencies and Capabilities, Networks, The Competitive Environment and The Opportunity Framework
03. The Transformation of Asia in a Global Changing Environment
04. Thrombin: Function and Pathophysiology
05. Interdisciplinary Approaches to Neuroscience Epistemology and Cognition
06. Honey: Current Research and Clinical Applications
07. Australia, Japan and Southeast Asia: Early Post-War Initiatives in Regional Diplomacy
08. Georgian History
09. Portugal: Economic, Political and Social Issues
10. Cancer Metastasis Research: Pathological Insight
11. Pediatric Cancer
12. Nephropathy: Diagnosis and Treatment

Newcastle,Callaghan,Australia and others)

Chapter 6. Extended Wavelet Transform for Discretely Sample Data;pp. 125-155

(Robert W.Johnson,Alphawave Research, Atlanta,Ga.,USA)

Chapter 7. Characterization and Classification of Agri-Food Products by Wavelet Signal Analysis;pp. 157-172

(C.B. Singh and Digvir S. Jayas,University ofManitoba,Winnipeg,Canada)

Chapter 8. Wavelet Transform in Banach Space and Quantum Tomography;pp. 173-221

(M. Rezaei, M. A. Jafarizadeh and M. Mirzaee,Tabriz University, Iran and others)

Chapter 9. Automatic Modeling of Discrete Wavelet Transforms Using Particle Swarm Optimization;pp. 223-243

(Marcus V.M. Figueredo, A. Beckert Neto, S.R. Rogal Jr and J.C. Nievola, Pontificia Universidade Catolica do Parana, Parana,Brazil)

Chapter 10. Wavelet Neural Networks - Innovative Processing Strategy for Classification and Quantification Models;pp. 245-268

(Juan Manuel Gutiérrez, Roberto Muñoz and Manel del Valle,Dept. of Electrical Engineering,Bioelectric Section,CINVESTAV., Mexico and others)

Chapter 11. Wavelets and Frames in Walsh Analysis;pp. 269-307

(Yuri A. Farkov, Dept. of Mathematics,Russian State Geological Prospecting University, Moscow)

Chapter 12. Stable Algorithm for Computation of Hankel Transform using Chebyshev Wavelets;pp. 309-334

(Rajesh K. Pandey, Vineet K. Singh and Om P. Singh, Indian Institute of Information Technology Design and Manufacturing,Jabalpur, India and others)

Chapter 13. Applications Of Wavelets In Financial Portfolio Optimization;pp. 335-364

(N.C.Suganya and G.A.Vijayalakshmi Pai, PSG College of Technology,Coimbatore,India)

Chapter 14. Three- Dimensional Estimation in 1-D Wavelet Profilometry by establishing a comparison between Phase Unwrapping Algorithms;pp. 365-381

(Jesús Carlos Pedraza-Ortega, Efren Gorrostieta-Hurtado, Marco A. Aceves Fernandez, Sandra L. Canchola-Magdaleno, Juan Manuel Ramos-Arreguin, Saul Tovar-Arrigaga, Emilio Vargas-Soto and Artemio Sotomayor-Olmedo, Universidad Autonoma de Queretaro,Mexico)

Chapter 15. Diffusion Wavelet for Efficient Real-time Monitoring of Acoustic Emission Signal in Nanomanufacturing;pp. 383-394

(Rajesh Ganesan, Dept. of Systems Engineering and Operations Research,George Mason University,Fairfax,VA USA)

Index

Series:

Mathematics Research Developments

Binding: Hardcover

Pub. Date: 2012 1st quarter

Pages: 7 x 10 (NBC - C) 401pp.

ISBN: 978-1-62100-252-9

Status: AV

Status Code	Description
AN	Announcing
FM	Formatting
PP	Page Proofs
FP	Final Production
EP	Editorial Production
PR	At Prepress
AP	At Press
AV	Available



Friday 26 October, 2012

Nova Science Publishers
© Copyright 2004 - 2012

Chapter 14

**THREE- DIMENSIONAL ESTIMATION IN 1-D
WAVELET PROFILOMETRY BY ESTABLISHING A
COMPARISON BETWEEN PHASE UNWRAPPING
ALGORITHMS**

*Jesús Carlos Pedraza-Ortega**, *Efren Gorrostieta-Hurtado*,
Marco A. Aceves Fernandez, *Sandra L. Canchola-Magdaleno*,
Juan Manuel Ramos-Arreguin, *Saul Tovar-Arrigaga*,
Emilio Vargas-Soto and Artemio Sotomayor-Olmedo
Facultad de Informatica, Universidad Autonoma de Queretaro, Mexico

Abstract

Three-dimensional (3-D) surface shape measurement and sensing by using a projected fringe pattern has been widely used considering the Transform Based profilometry. Several articles show that these methods require a single image with a sinusoidal fringe pattern projected on it. Usually, the projected pattern has a known spatial frequency and this information is used to avoid discontinuities in the fringes with high frequency. Among single projected fringe pattern, most of the methods use Fourier or Wavelet transforms to extract the phase information. However, they focused only on the transform method and not on the phase unwrapping algorithms. It is well known that wavelet transforms are used to analyze signals whose frequency contents varies over the duration of the signal (wrapped phase), also, wavelet techniques provide a flexible, elegant, and a computational efficient solution to these type of problems. In this work, a 1-D wavelet profilometry method is presented considering two different wavelet transforms. Later, different phase unwrapping algorithms are used to extract the depth information considering local and global analysis. Several computer simulations and experiments are carried out to validate the proposed method. The merits and limitations of each of these variations on the method are indicated and the error is estimated.

* E-mail address: caryoko@yahoo.com

1. Introduction

Since a few years ago, the 3D information of an object is required and the main idea is to extract the depth information from an image or set of images in an efficient and automatic way. As a result of the process, the useful depth information can be used in several tasks such as synthetic aperture radar (SAR), automatic inspection, reverse engineering, 3D robot navigation magnetic resonance imaging (MRI), optical metrology, interferometry and so on [1]. Among all the contact measurement techniques to carry out this process, the most widely used are a vision-based system together with a tool which is in contact with the object, like laser, fringe projection and so on. Moreover, the most widely used is the fringe projection. The fringe processing methods are widely used because of its characteristics like high accuracy, noise-immunity and fast processing speed. Inside the fringe projection methods, the mostly used and known is the Fourier Transform Profilometry (FTP) method [2], Phase-shifting or phase stepping [3, 4], digital phase locked loop [5], direct phase detection [6], and a variation of the FTP method, the one called Wavelet Transform Profilometry [12, 16]. One of the main challenges of the previously mentioned methods is the problem statement of the wrapped phase information caused by the fact that the phase of a periodically varying intensity pattern is encoded or wrapped and it contains the depth information of the object. The phase unwrapping problem has been tackled by several researchers in the past; dozens of algorithms are fully dedicated to solve this problem in many ways. One of the first algorithms to deal with this problem was proposed by Takeda and Mutoh in 1982 [2], which used a single phase unwrapping algorithm. Later Berryman [7] and Pedraza [8, 17, 18] proposed a modified Fourier Transform Profilometry by carrying out global and local analyses as a solution of the phase wrapped information. Then, unwrapping algorithms (temporal and spatial) were introduced and modified [7-10]. Phase unwrapping techniques use exhaustive data computations and approximations; however, these approaches have a slight contribution to understand the cause of failure in the phase unwrapping process. This research presents an implementation of phase unwrapping algorithms, considering the problem of residues.

Generally, most of the cited methods used a Modified Fourier Transform Profilometry, and another suitable solution is to use the wavelet transform to extract the phase information.

Wavelet transform too offers multi-resolution in time and space frequency, and it is an alternative that offers some advantages over the Fourier transform [9-10]. Using a wavelet transform can carry out the fringe pattern analysis. The main idea of this analysis consists in demodulating the deformed fringe patterns and extracting the phase information encoded into it, therefore estimate the height profile of the object quite similar to Fourier transform.

Different wavelet algorithms are used in the demodulation process to extract the phase of the deformed fringe patterns. Those algorithms can be classified into two categories: phase estimation and frequency estimation techniques. The phase estimation algorithm uses a complex mother wavelet, here, the extracted phase is wrapped into 2π discontinuities consequently a phase unwrapping algorithm is required to remove these 2π jumps. Zhong et al. [9] have applied Gabor wavelets to extract the phase distribution where a phase unwrapping algorithm is required. The frequency estimation technique estimates the instantaneous frequencies in a fringe pattern, which are then integrated to estimate the phase. The phase extracted using this technique is continuous; consequently, phase unwrapping algorithms are not required for 2D Wavelet Profilometry. Complex or real mother wavelet

can be used to estimate the instantaneous frequencies in the fringe pattern. Dursun et al. [14] and Afifi et al. [15] have used Morlet or Paul wavelets, separately, to obtain the phase distribution of projected fringes. Also, Gdeisat et al. [16] have proposed a 1D continuous wavelet transform approach to retrieve phase information in temporally and spatially fringe patterns.

Most of the previous research are focused on using the Fourier and wavelet transforms to obtain the 3D information from an object; pre-filtering the images, extracting the phase information of fringe patterns, using phase unwrapping algorithms, and so on.

In the present research, a comparison between two phase unwrapping algorithms is presented in 1D Wavelet Profilometry, implemented in order to obtain the 3D information from an object. First, the spatial frequency of the projected fringe pattern is obtained; later the mathematical model is obtained and used together with the spatial frequency in order to establish the problem. Then, a 1D Wavelet Profilometry is applied considering the most suitable wavelets for the fringe analysis. Later, two phase unwrapping algorithms are used to obtain the desired 3D information. One contribution in this research is the proposed methodology, because in previous works there are no comparisons among different phase unwrapping (PU) methods in 1D Wavelet based profilometry. The results show that it's suitable to compare the present work with other similar researches. To test the method, some virtual objects were created for use in computer simulations and also some experiments were carried out.

2. Profilometry Basics

As were described early, there are several fringe projection techniques that are used to extract the three-dimensional information from the objects. The most widely used techniques are Fourier Transform Profilometry and Wavelet Profilometry, which are presented in this work.

2.1. Fourier Transform Profilometry (FTP)

The projected fringe pattern and an object with projected fringes on it, as shown on figure 3, can be represented as:

$$g(x, y) = a(x, y) + b(x, y) * \cos[2 * \pi f_0 x + \varphi(x, y)] \quad (1)$$

$$g_o(x, y) = a(x, y) + b(x, y) * \cos[2 * \pi f_o x + \varphi_o(x, y)] \quad (2)$$

where $g(x,y)$ and $g_o(x,y)$ are the intensities of the images at the point (x,y) , $a(x,y)$ represents the background illumination, $b(x,y)$ is the contrast between the light and dark fringes, f_o is the spatial-carrier frequency and $\varphi(x,y)$ and $\varphi_o(x,y)$ are the corresponding phase to the fringe and distorted fringe pattern.

The phase $\varphi(x,y)$ contains the desired information. This angle $\varphi(x,y)$ is the phase shift caused by the object surface end the angle of projection, and its expressed as:

$$\varphi(x, y) = \varphi_0(x, y) + \varphi_z(x, y) \tag{3}$$

where $\varphi_0(x,y)$ is the reference plane projected phase angle, and $\varphi_z(x,y)$ is the object’s height distribution phase.

In Pedraza et al work [17, 18], the Equation 3 can be rewritten as:

$$\varphi_z(x, y) = \frac{h(x, y)2\pi f_0 d_0}{h(x, y) - l_0} ; h(x, y) = \frac{l_0 \phi_z(x, y)}{\phi_z(x, y) - 2\pi f_0 d_0} \tag{4}$$

where the value of $h(x,y)$ is measured and considered as positive to the left side of the reference plane. Also, the Equation 4 expresses the height distribution as a function of the phase distribution.

The Equation 1 can be rewritten as:

$$g(x, y) = \sum_{n=-\infty}^{\infty} A_n r(x, y) \exp(in\varphi(x, y)) * \exp(i2\pi f_0 x) \tag{5}$$

where $r(x,y)$ is the reflectivity distribution on the diffuse object [3,4]. Then, a *FFT* (Fast Fourier Transform) is applied to the signal in the x direction only. Thus, the following equation is obtained:

$$G(f, y) = \sum_{-\infty}^{\infty} Q_n(f - nf_0, y) \tag{6}$$

where Q_n is the 1D Fourier Transform of $A_n \exp[in\varphi(x,y)]$.

Here $\varphi(x,y)$ and $r(x,y)$ vary very slowly in comparison with the fringe spacing, then the Q peaks in the spectrum are separated from each other. It is also necessary to consider that if a high spatial fringe pattern is chosen, the *FFT* will have a wider spacing among the frequencies; this behavior helps to identify the fundamental peak f_0 . In *FTP*, next step is to remove all signals but positive fundamental peak f_0 . Then, the result is shifted and centered. Later, the *IFFT* (Inverse Fast Fourier Transform) is applied in the x direction only. Here, is necessary to separate the phase part of the result from the rest because it contains the depth information:

$$\begin{aligned} \varphi_z(x, y) &= \varphi(x, y) + \varphi_0(x, y) \\ &= \text{Im}\{\log(g(x, y)g_0^*(x, y))\} \end{aligned} \tag{7}$$

The whole phase map is obtained by applying the same procedure for each x line. The result is that the values of the phase map are wrapped at some specific values whose range lie between π and $-\pi$. Then, to recover the true phase it is necessary to restore the measured wrapped phase by an unknown multiple of $2\pi f_0$ [17]. However, to analyze and describe signals, it requires information from both domains time and frequency, therefore Fourier is not a suitable solution to express those signals and another way is proposed, wavelet transform.

2.2. Wavelet Transform Profilometry

The wavelet transform (WT) is considered an appropriate tool to analyze non-stationary signals. This technique has been developed as an alternative approach to the most common transforms, such as Fourier transform, to analyze fringe patterns. Furthermore, WT has a multi-resolution property in both time and frequency domains which solves a commonly know problem in other transforms like the resolution.

A wavelet is a small wave of limited duration (this can be real or complex). For this, two conditions must be satisfied: firstly, it must have a finite energy. Secondly, the wavelet must have an average value of zero (admissibility condition). It is worth noting that many different types of mother wavelets are available for phase evaluation applications. The most suitable mother wavelet is probably the complex Morlet one[2]. The Morlet wavelet is a plane wave modulated by a Gaussian function, and is defined as:

$$\psi(x) = \pi^{1/4} \exp(icx) \exp(-x^2 / 2) \tag{8}$$

where c is a fixed spatial frequency, and chosen to be about 5 or 6 to satisfy an admissibility condition [11]. Figure 1 shows the real part (dashed line) and the imaginary part (solid line) of the Morlet wavelet.

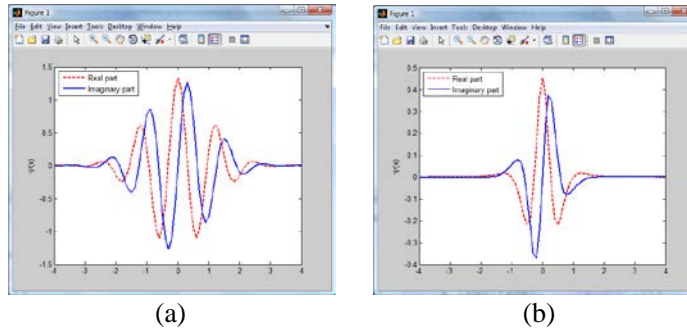


Figure 1. Mother wavelets: (a) Complex Morlet and (b) Paul.

Also, Paul Wavelet is considered as one choice to perform the phase evaluation and is defined as:

$$\psi(x) = \frac{2^n n! (1-ix)^{-(n+1)}}{2\pi \sqrt{\frac{(2n)!}{2}}} \tag{9}$$

where n is the order of the Paul mother wavelet and chosen to have the value of 5.

The one-dimensional continuous wavelet transform (1D-CWT) of a row $f(x)$ of a fringe pattern is obtained by translation on the x axis by b (with y fixed) and dilation by s of the mother wavelet $\psi(x)$ as given by:

$$W(s, b) = \frac{1}{\sqrt{s}} \int_{-\infty}^{\infty} f(x) \psi^* \left(\frac{x-b}{s} \right) dx \tag{10}$$

here, * denotes complex conjugation and $W(s,b)$ is the calculated CWT coefficients which refers to the closeness of the signal to the wavelet at a particular scale.

In this research, the phase estimation and frequency estimation methods are used to extract the phase distribution from two dimensional fringe patterns. In the phase estimation method, a complex Morlet and Paul wavelets will be applied to a row of the fringe pattern. The resultant wavelet transform is a two dimensional complex array, where the phase arrays can be calculated as follows:

$$abs(s,b) = |W(s,b)| \quad (11)$$

and

$$\varphi(s,b) = \tan^{-1} \left(\frac{\Im\{W(s,b)\}}{\Re\{W(s,b)\}} \right) \quad (12)$$

To compute the phase of the row, the maximum value of each column of the modulus array is determined and then its corresponding phase value is found from the phase array. By repeating this process on all rows of the fringe pattern, a wrapped phase map results and an unwrapping algorithm is then needed to unwrap it.

In the frequency estimation method, a complex Morlet wavelet and Paul wavelet are applied to a row of the fringe pattern. The resultant wavelet transform is a two dimensional complex array. The modulus array can be found using Equation (13) and hence the maximum value for each column and its corresponding scale value can be determined. Considering that we are interested in the 1D signal:

$$f(x) = a(x) + b(x) \cos(2\pi f_0 x + \varphi(x)) \quad (13)$$

Considering the Euler identity for $\cos(x)$, then the Equation 13 could be re-formulated as:

$$f(x) = a(x) + b(x) \cos(\varphi(x)) = a(x) + b(x) \frac{e^{i\varphi(x)}}{2} + b(x) \frac{e^{-i\varphi(x)}}{2} \quad (14)$$

The analytic function f in an open interval A , where $z_0 \in A$ can be decomposed into Taylor series:

$$f(z) = \sum_{k=0}^{\infty} \frac{f^{(k)}(z_0)}{k!} (z - z_0)^k \quad (15)$$

Therefore:

$$\varphi(x) = \varphi(x) + \varphi'(x)(b)(x-b) + \frac{\varphi''(x)}{2!}(x-b)^2 + \frac{\varphi'''(x)}{3!}(x-b)^3 + \dots \quad (16)$$

Considering:

$$\varphi(x) = \varphi(b) + \varphi''(b) \approx 0, \varphi'''(b) \approx 0, \varphi^{(4)}(b) \approx 0, \dots, \varphi^{(k)}(b) \approx 0 \quad (17)$$

Then, the function can be reduced as:

$$\varphi(x) = \varphi(b) + \varphi'(b)(x - b) \quad (18)$$

Moreover, the Morlet Wavelet is defined in the Equation (8) this wavelet will be applied to the mother wavelet, as shown in Equation (10):

If $s = 1$, then:

$$\begin{aligned} W(s, b) &= \frac{1}{s} \int_{-\infty}^{\infty} f(x) \psi^* \left(\frac{x-b}{s} \right) dx \\ &= \int_{-\infty}^{\infty} \left[a(x) + b(x) \frac{e^{i\varphi(x)}}{2} + b(x) \frac{e^{-i\varphi(x)}}{2} \right] \psi^* \left(\frac{x-b}{s} \right) dx \\ &= a \int_{-\infty}^{\infty} \psi^* \left(\frac{x-b}{s} \right) dx + \frac{b}{2} \int_{-\infty}^{\infty} \frac{e^{i[\varphi(b)+\varphi'(b)(x-b)]}}{2} \psi^* \left(\frac{x-b}{s} \right) dx + \frac{b}{2} \int_{-\infty}^{\infty} \frac{e^{-i[\varphi(b)+\varphi'(b)(x-b)]}}{2} \psi^* \left(\frac{x-b}{s} \right) dx \end{aligned} \quad (19)$$

By solving Equation 19, the following equation is obtained:

$$a\sqrt{2\pi}e^{-\frac{1}{2}\sigma_0^2} + \frac{b}{2}\sqrt{2\pi}e^{-\frac{1}{2}(\sigma_0+s\sigma_s)^2}e^{-i\sigma_s b} + \frac{b}{2}\sqrt{2\pi}e^{-\frac{1}{2}(\sigma_0-s\sigma_s)^2}e^{i\sigma_s b} \quad (20)$$

Then the instantaneous frequencies are computed using the next Equation [11]:

$$\hat{f}(b) = \frac{c + \sqrt{c^2 + 2}}{2s_{\max}(b)} - 2\pi f_o \quad (21)$$

where f_o is the spatial frequency. At the end, the phase distribution can be extracted by integrating the estimated frequencies.

The same procedure can be developed to get the instantaneous frequencies, which lead us to have the wrapped phase map and therefore it is necessary to apply a phase unwrapping algorithm.

3. Phase Unwrapping

Since two decades ago, phase unwrapping has been a research area and many papers have been published, presenting some ideas that solves the problem. Several phase unwrapping algorithms have been proposed, implemented and tested.

The phase unwrapping process is not a trivial problem due to the presence of phase singularities (points in 2D, and lines in 3D) generated by local or global undersampling. The correct 2D branch cut lines and 3D branch cut surfaces should be placed where the gradient of the original phase distribution exceeded π rad value. However, this important information is lost due to undersampling and cannot be recovered from the sampled wrapped phase distribution alone. Also, is important to notice that finding a proper surface, or obtaining a minimal area or using a gradient on a wrapped phase will not work and one could not find the correct branch in cut surfaces.

The phase unwrapping has many applications in applied optics that require an unwrapping process, and hence many phase unwrapping algorithms has been developed specifically for data with a particular application. Moreover, there is no universal phase unwrapping algorithm that can solve wrapped phase data from any application. Therefore, phase unwrapping algorithms are considered as a trade-off problem between accuracy of solution and computational requirements. However, even the most robust and complete phase unwrapping algorithm cannot guarantee in giving successful or acceptable unwrapped results without a good set of initial parameters. Unfortunately, there is no standard or technique to define the parameters that guarantee a good performance on phase unwrapping.

To face the phase unwrapping problems, algorithms can be divided in two main categories: local and global phase unwrapping. Local phase unwrapping algorithms find the unwrapped phase values by integrating the phase along a certain path[6].

Global phase unwrapping algorithms locate the unwrapped phase by minimizing a global error function and are also called local phase unwrapping algorithm and a global phase unwrapping algorithm, by following the methodology proposed by Pedraza in [1]. The unwrapped phase values and the wrapped phase can be related with each other as:

$$\Psi(n) = \varphi(n) + 2\pi k(n)$$

$$\text{With constraints} \quad -\pi < \Psi(n) \leq \pi \quad (22)$$

$$-\pi < \Psi(n) \leq \pi$$

And:

$$\varphi(n) = \Psi(n) + 2\pi v(n)$$

$$\text{with constraints} \quad -\infty < \varphi(n) \leq \infty \quad (23)$$

$$-\infty < \varphi(n) \leq \infty$$

Here $\Psi(n)$ holds the wrapped phase values and $\varphi(n)$ holds the unwrapped phase values, $k(n)$ is the function containing the integers that must be added to the wrapped phase φ to be unwrapped, n is an integer and $v(n)$ is the function containing a set of integers that must be added to the wrapped phase Ψ .

The wrapping operation ω , which converts the unwrapped phase, is defined by:

$$\omega\{\phi(n)\} = \arctan \left[\frac{\sin(\phi(n))}{\cos(\phi(n))} \right] \quad (24)$$

3.1. Local Phase Unwrapping

Local phase unwrapping algorithms finds the unwrapped phase values by integrating the phase along certain path that covers the whole wrapped phase map. The local phase unwrapping defines the quality of each pixel in the phase map to unwrap the highest quality pixels first and the lowest quality pixels last (quality-guided phase unwrapping). For this purpose, the methods known as residue-balancing are proposed, which attempts to prevent error propagation by identifying residues (the source of noise in the wrapped phase). The residues must be balanced and isolated by using barriers (branch-cuts), therefore, it aims to

produce a path-independent wrapped phase map. Path-dependency occurs to the existence of residues.

Residue-balancing algorithms search for residues in a wrapped-phase map and attempt to balance positive and negative residues by placing cut lines between them to prevent the unwrapping path breaking the mesh created. The residue is identified for each pixel in the phase map by estimating the wrapped gradients in a 2×2 closed loop, as shown in Figure 2.

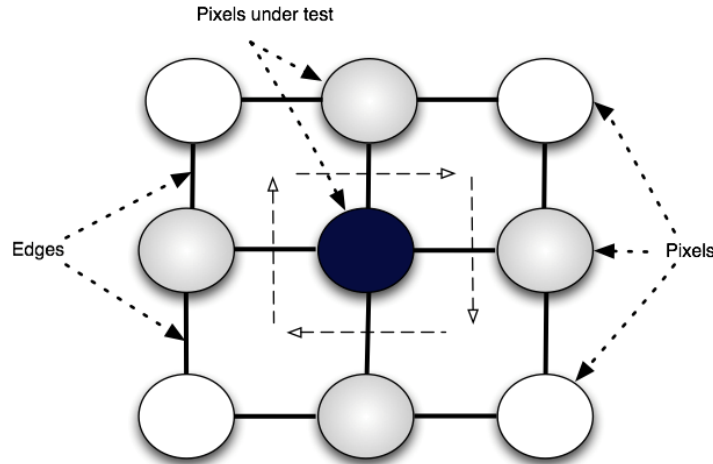


Figure 2. Identifying residues in a 2×2 closed path.

This is carried out using the following equation:

$$r = \Re \left[\frac{\Psi_{i,j} - \Psi_{i+1,j}}{2\pi} \right] + \Re \left[\frac{\Psi_{i+1,j} - \Psi_{i+1,j+1}}{2\pi} \right] + \Re \left[\frac{\Psi_{i,j+1} - \Psi_{i,j}}{2\pi} \right] + \Re \left[\frac{\Psi_{i,j+1} - \Psi_{i,j+1}}{2\pi} \right] \quad (25)$$

Where $\Re[\]$ rounds its argument to the nearest integer, $\Psi_{x,y}$ is the wrapped pixel. The equation 25 can only take three possible results: 0, +1, and -1. A pixel under test is considered to be a positive residue if the value of r is +1, and it is considered to be a negative residue if the value is -1. Conversely, the pixel is not a residue if the value of r is zero. After identifying all residues in the wrapped phase map, these residues have to be balanced by means of branch cuts. Branch-cuts act as barriers to prevent the unwrapping path going through them. If these branch cuts are avoided during the unwrapping process, no errors propagate and the unwrapping path is considered to be path independent. On the other hand, if these branch cuts are penetrated during the unwrapping, errors propagate throughout the whole phase map, and in this case the unwrapping path is considered to be path dependent.

3.2. Global Phase Unwrapping

In the previous section, it was stated that local phase unwrapping algorithms follow a certain unwrapping path in order to unwrap the phase. They begin at a grid point and integrate the wrapped phase differences over that path, which ultimately covers the entire phase map.

Local phase unwrapping algorithms (residue-balancing algorithms) generate branch cuts and define the unwrapping path around these cuts in order to minimize error propagation.

In contrast, global phase unwrapping algorithms formulate the phase unwrapping problem in a generalized minimum-norm sense [6]. Global phase unwrapping algorithms attempt to find the unwrapped phase by minimizing the global error function as shown in equation 26

$$\varepsilon^2 = ||\text{solution} - \text{problem} ||^2 \tag{26}$$

Global phase unwrapping algorithms seek the unwrapped phase whose local gradients in the x and y direction match, as closely as possible and shown in figure 3.

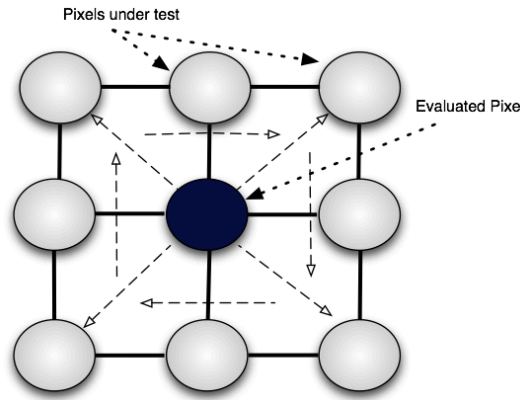


Figure 3. Matching pixel gradients in x and y direction.

$$\varepsilon^2 = \sum_{i=0}^{M-2} \sum_{j=0}^{N-1} |\Delta^x \varphi(i, j) - \hat{\Delta}^x \psi(i, j)|^p + \sum_{i=0}^{M-1} \sum_{j=0}^{N-2} |\Delta^y \varphi(i, j) - \hat{\Delta}^y \psi(i, j)|^p \tag{27}$$

Where $\Delta^x \varphi(i, j)$ and $\Delta^y \varphi(i, j)$ are unwrapped phase gradients in the x and y directions respectively, which are given by:

$$\Delta^x \varphi(i, j) = \varphi(i+1, j) - \varphi(i, j) \tag{28}$$

$$\Delta^y \varphi(i, j) = \varphi(i, j+1) - \varphi(i, j) \tag{29}$$

$\hat{\Delta}^x \psi(i, j)$, $\hat{\Delta}^y \psi(i, j)$ and $\tilde{\Delta}^x \psi(i, j)$ are the wrapped values of the phase gradients in the x and y directions respectively, and they are given by:

$$\hat{\Delta}^x \psi(i, j) = \omega \{ \psi(i+1, j) - \psi(i, j) \} \tag{30}$$

$$\hat{\Delta}^y \psi(i, j) = \omega \{ \psi(i, j+1) - \psi(i, j) \} \tag{31}$$

Finally, the wrapping operator defined in Equation (24) is applied.

4. Setup and Proposed Methodology

Considering Figure 4, we have a fringe pattern, which is projected from the projector; the fringe reaches the object at point H and will cross the reference plane at the point C. By observation, the triangles $D_p H D_c$ and CHF are similar and since:

$$\frac{CD}{-h} = \frac{d_0}{l_0} \quad (32)$$

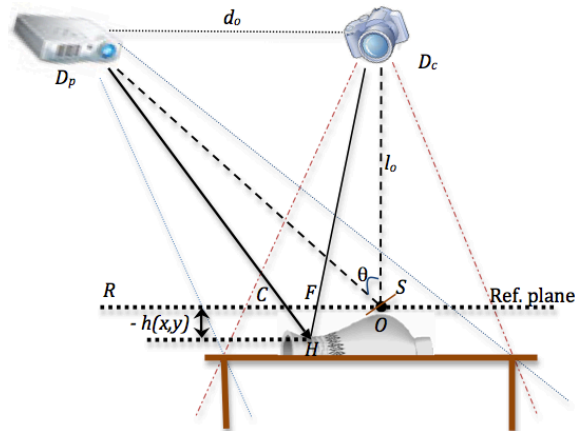


Figure 4. Experimental setup.

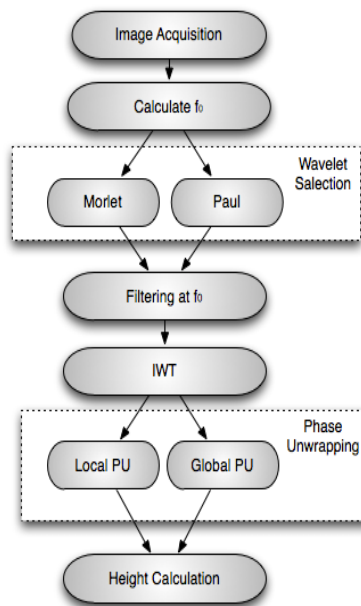


Figure 5. Proposed methodology.

The experimental setup shown in Figure 4 is proposed and during the experiments the methodology in Figure 5 is applied. The first step is to acquire the image. Due to the nature of the image, sometimes a filtering to eliminate the noise is necessary, and a filter is used. Next, the fundamental frequency f_0 is estimated. Later, the mother is selected (Morlet or Paul) and applied. The filter at f_0 is carried out and the Inverse Wavelet transformation is done. At this stage, the information of the height is phase wrapped and two phase unwrapping algorithms are proposed: Local and Global Analysis Algorithm and Graph Cuts Algorithm. The final step is to obtain the object reconstruction and in some cases to determine the error (in case of virtual created objects). The experimental setup uses a high-resolution digital CCD camera and a high resolution digital projector.

The object of interest can be any three-dimensional object and for this work, three objects are considered, which are shown on figure 6.

It is also important to develop software able to produce several different fringe patterns. To create several patterns, it is necessary to modify the spatial frequency (number of fringes per unit area), and resolution (number of levels to create the sinusoidal pattern) of the fringe pattern. It may also be necessary to include into the software development a routine capable of performing phase shifting as well as to include the horizontal or vertical orientation projection of the fringe pattern.

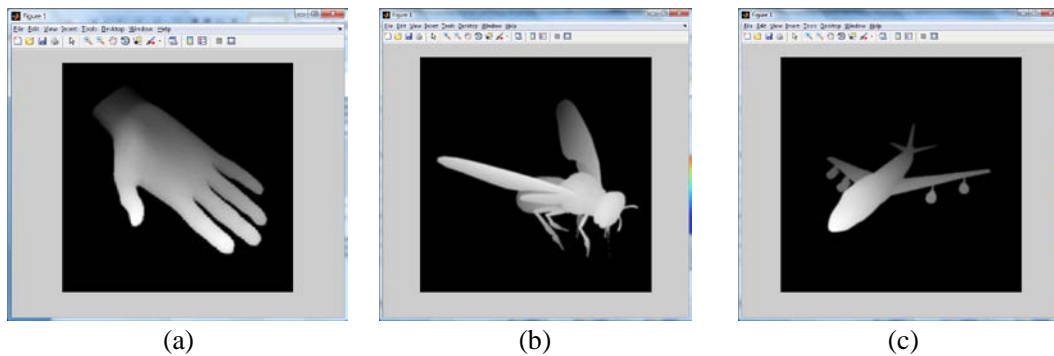


Figure 6. Virtual objects used in the test: (a) Hand, (b) Fly, and (c) Airplane.

5. Results

To test the methodology, first an object with Hand shape is used. Then, a sinusoidal fringe pattern of known spatial frequency is created with 128 fringes and added to the shape of the created object. The resulting image is shown in Figure 7(c). It is worth noting the distortions of the fringe pattern due to the object's shape.

The wrapped phase and its mesh are shown in Figure 8. The reconstructed Hand using the Morlet Wavelet Transform and applying the Local PU Analysis and the Global PU Analysis can be seen in Figure 9. Notice that, by applying this method, the shape of the Hand looks almost equal, but it has an error magnitude around 3.2 and 2.1% respectively.

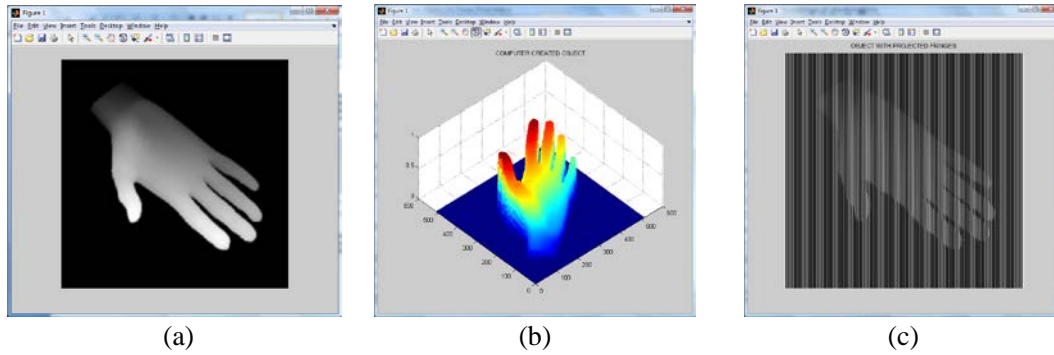


Figure 7. Computer created Hand: (a) Object image, (b) Object mesh, and (c) fringes projected on it.

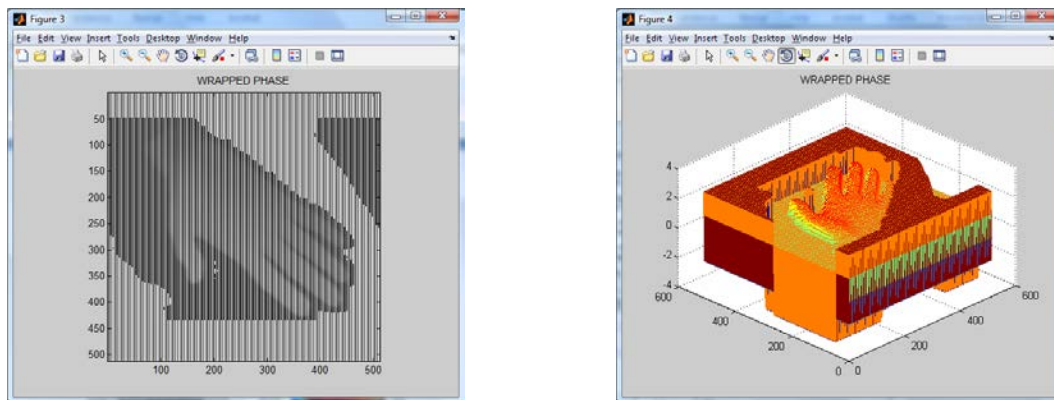


Figure 8. Wrapped phase (image and mesh).

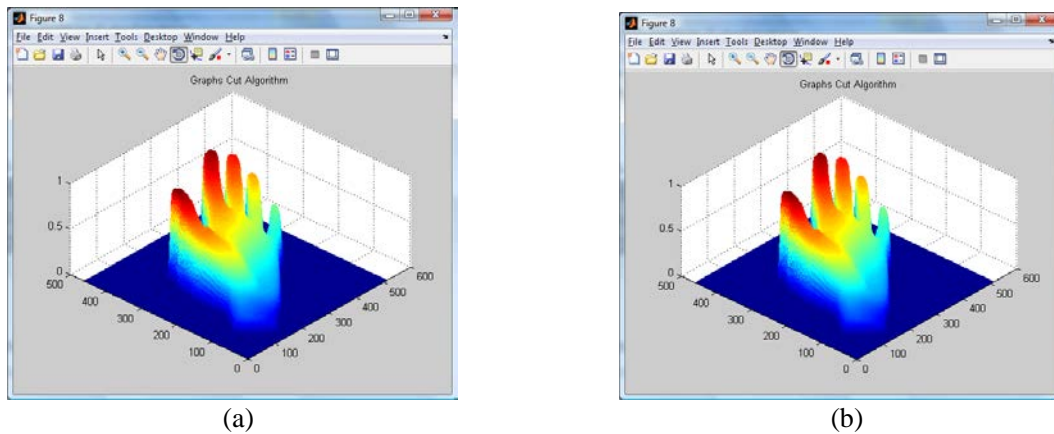


Figure 9. Reconstructed objects by using Morlet Wavelet and (a) Local Phase Unwrapping Algorithm, and (b) Global Phase Unwrapping Algorithm.

The results on Figure 9 show that the whole volume presents an acceptable error and the shape is well defined. The mother wavelet used was the Morlet but the same experiment was conducted for the Paul wavelet and the results obtained were similar to those presented on

figure 9. The computer simulation allowed us to test the proposed methodology. On Figures 7, 8 and 9 the results of the methodology are presented step by step.

To validate the whole methodology, more experiments were conducted considering the objects observed on Figure 6(b) and (c). Those objects have different shapes (computer created), where the height is known in every point in the object. Then, the Morlet and Paul mother Wavelets are considered as well as the two different phase unwrapping algorithms. As a second experiment, Paul Wavelet is used and height of the virtual object was compared with each one of the analysis and the results are presented in figure 9.

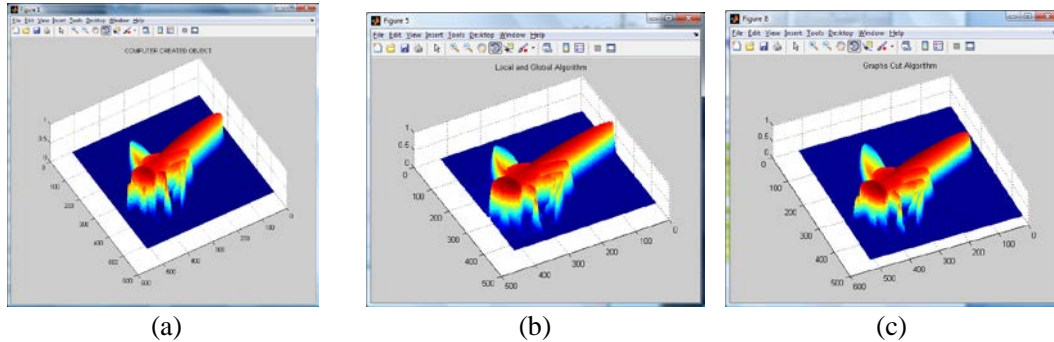


Figure 9. Fly object and its reconstruction using Paul Wavelet: (a) Object, (b) Local PU Algorithm, and (c) Global PU Algorithm.

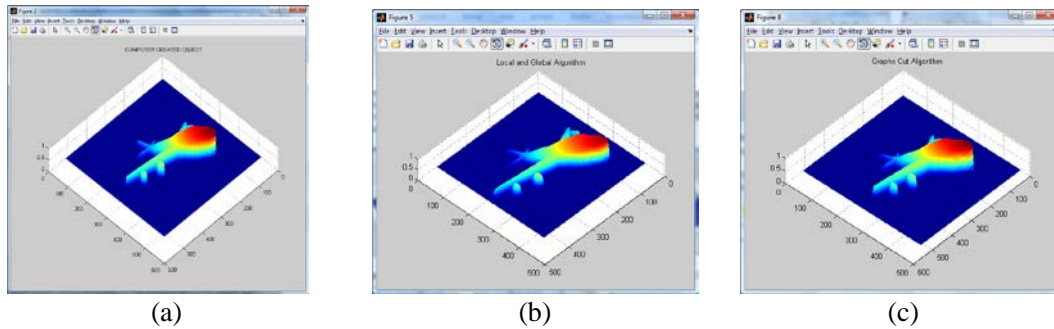


Figure 10. Airplane object and reconstruction using Morlet Wavelet: (a) Object, (b) Local PU Algorithm, and (c) Global PU Algorithm.

Third experiment was conducted with Morlet Wavelet and the object used was the airplane, and the respective results of the reconstruction process can be seen in Figure 10. Later, all the experiments are joined and the error magnitude is enclosed on tables 1 and 2. The results show that the better performance was obtained by using the Morlet wavelet together with the Global Phase Unwrapping Algorithms in final step to perform the 3D reconstruction process.

Finally, the performance of the proposed methodology was tested in a real object (a volleyball's ball) and both Morlet and Paul wavelets were used considering the Global Phase Unwrapping Algorithm for the phase unwrapping and the results are observed in Figure 11.

Table 1. Error table using Morlet Wavelet.

Object	Local PU	Global PU
Hand	3.26	2.11
Fly	3.47	2.21
Airplane	3.51	2.18

Table 2. Error table using Paul Wavelet.

Object	Local PU	Graph PU
Hand	4.37	3.43
Fly	4.65	3.76
Airplane	4.71	3.55

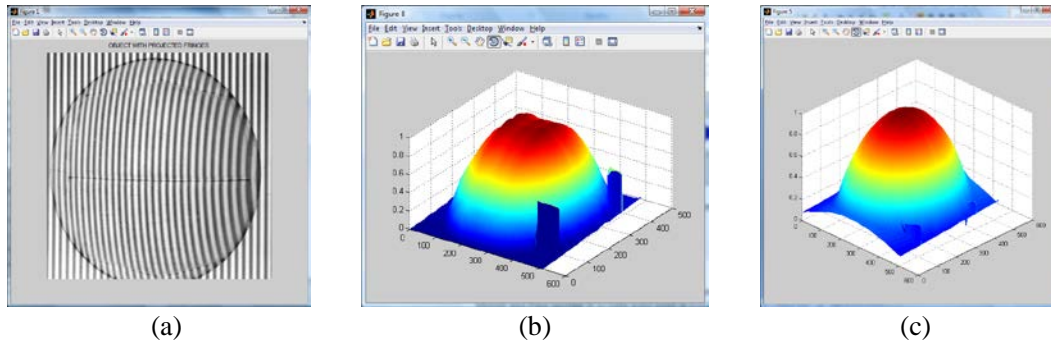


Figure 11. Real object and reconstruction: (a) Object, (b) Using Morlet Wavelet, and (c) Paul Wavelet with Graph Cuts Algorithm.

Table 3. Error table analysis of real object.

Object	Wavelet	Local PU	Global PU
Volleyball's ball	Morlet	4.51	3.24
Volleyball's ball	Paul	4.49	3.13

6. Conclusions and Future Work

In this work, an enhanced wavelet based Profilometry was presented and tested. Both Morlet and Paul mother wavelets were used in conjunction with local and global methods, in the phase unwrapping process. Three different objects generated by the computer were utilized (hand, fly and airplane). The object's projected fringe pattern has a known spatial frequency. Additionally, a real object was taken in order to implement the proposed methodology and accurate reconstruction of the object. Among the proposed wavelets, the one who shown better performance was Morlet wavelet over Paul wavelet, since Morlet was the one that produced a minimal error. As a conclusion, we can say that the proposed

methodology could be used to digitize diverse objects with good results. As a future work, the software performance can be improved in order to implement it inside an embedded system.

References

- [1] Gokstorp, M. Depth Computation in Robot Vision, Ph.D. Thesis, *Department of Electrical Engineering*, Linkoping University, Linkoping, Sweden, (1995).
- [2] M. Takeda, H. Ina and S. Kobayashi, *J. Opt. Soc. Am.* **72**, 156 (1982).
- [3] J.E. Grevenkamp and J.H. Bruning, Phase-shifting interferometry. In D. Malacara (Ed.), *Optical Shop Testing*, Wiley, New York (1992).
- [4] K. Creath, in: W.R. Robinson and G.T. Reid (Eds.), *Interferogram Analysis: Digital Fringe Pattern Measurement Techniques*, Institute of Physics, Philadelphia, PA (1993).
- [5] M. Gdeisat, D. Burton, M. Lalor, *Appl. Opt.* **39**, 5326 (2000).
- [6] Y. Ichioka, M. Inuiya, *Appl. Opt.* **11**, 1507 (1972).
- [7] F.Berryman, P. Pynsent, J. Cubillo, *Opt. Lasers Eng.* **39**, 35 (2003).
- [8] J.C. Pedraza, Image Processing for 3D Reconstruction using a Modified Fourier Transform Profilometry Method, *Lecture Notes on Artificial Intelligence*, Springer-Verlag, Berlin, (2007) pp. 705.
- [9] P.K. Rastogi, *Digital Speckle Pattern Interferometry and Related Techniques*, Wiley, New York (2001).
- [10] K. Itoh, *Appl. Opt.* **21**, 2470 (1982).
- [11] L.S. Wu, *J. Zhejiang Univ. Sci. A*, **7**, 1026 (2006).
- [12] J.G. Zhong, J.W. Wang, *Appl. Opt.* **43**, 4993 (2004).
- [13] Q. Zang, W.J.Chen, Y. Tang, *Opt. Commun.* **282**, 778 (2009).
- [14] A. Dursun, S. Ozder, N. Ecevit, *Meas. Sci. Tech.* **15**, 1768 (2004).
- [15] M. Afifi, A. Fassi-Fihri, M. Marjane, K. Nassim, M. Sidki and S. Rachafi, *Opt. Commun.* **211**, 47 (2002).
- [16] M.A. Gdeisat, D.R. Burton and M.J. Lalor, *Appl. Opt.* **45**, 8722 (2006).
- [17] J.C. Pedraza-Ortega, et al., Three-Dimensional Reconstruction System based on a Segmentation Algorithms and a Modified Fourier Transform Profilometry. *In Proceedings of the IEEE Electronics, Robotics and Automotive Mechanics Conference*, Cuernavaca, Morelos, September (2009).
- [18] J.C. Pedraza-Ortega, et al., A Profilometric Approach for 3D Reconstruction Using Fourier and Wavelet Transforms. *Lecture Notes on Artificial Intelligence*, Springer-Verlag, Berlin, pp. 313-323 (2009).
- [19] M.A. Gdeisat, D.R. Burton and M.J. Lalor, *Opt. Lasers Eng.* **47**, 1348 (2009).